Synthesis and Studies on 2-Hexylthieno[3,2-b]thiophene End-Capped Oligomers for OTFTs

Hyung-Sun Kim,[†] Yun-Hi Kim,*[,‡] Tae-Hoon Kim,[†] Yong-Young Noh,[§] Seungmoon Pyo,[||] Mi Hye Yi,[||] Dong-You Kim,[†] and Soon-Ki Kwon*[,†]

School of Nano & Advanced Materials Engineering and Engineering Research Institute and Department of Chemistry, Gyeongsang National University, Chinju 660-701, Korea, Department of Materials Science & Engineering, Gwangju Institute of Science and Technology, Gwangju 500-712, Korea, and Polymeric Nanomaterials Laboratory, Korea Research Institute of Chemical Technology, 100 Jang-dong, Daejeon 305-610, Korea

Received January 8, 2007. Revised Manuscript Received April 17, 2007

The new semiconductors that were composed of a naphthalene or anthracene core unit and alkylated thienothiophene on both sides, 2,6-bis(5′-hexyl-thieno[3,2-b]thiophen-2′-yl)naphthalene (DH-TNT) and 2,6-bis(5′-hexyl-thieno[3,2-b]thiophen-2′-yl)anthracene (DH-TAT), were synthesized by Suzuki coupling reaction. The obtained oligomers were characterized by FT-IR, mass and elemental analysis, UV−visible spectroscopy, cyclovoltammetry, differencial scanning calorimetry, and thermogravimetric analysis. Vacuum-evaporated films were characterized by X-ray diffraction and atomic force microscopy (AFM). They all form highly ordered polycrystalline vacuum-evaporated films. DH-TAT exhibits excellent field-effect performances, with a hole mobility of 0.14 cm^2/Vs, an on/off current ratio of 6.3×10^6, and a good threshold voltage of −14 V when it was deposited at $T_s = 120$ °C on HMDS-treated SiO_2. DH-TNT shows a hole mobility of 0.084 cm^2/Vs and an on/off current ratio of 8.8×10^5 when it was deposited at $T_s = 100$ °C.

Introduction

Organic thin film transistors (OTFTs) based on oligomers and polymers have recently received considerable attention because of their fundamental optoelectronic properties and potential applications for organic integrated circuit sensors,[1] low-cost memories, smart cards, and driving circuits for large-area display device applications such as active-matrix flat-panel liquid-crystal display (AMFPDs), organic light-emitting diodes, and electronic paper displays.[2,3] The field-effect mobility of OTFTs is still lower than those of the inorganic thin film transistors. However, the advantages of cheap manufacturing and simple processing make them suitable for commercial applications. The most important criteria for a commercial application of OTFTs are high charge-carrier mobility and high on/off current ratio. Among the rest, the facts important for obtaining high mobilities are the use of organic molecules with high structural order and an extended π system as active layers. Many of the organic semiconductors used for the fabrication of the p-channel in OTFTs have been derived from thiophene-based π-conjugated systems, oligothiophene,[4,5] carbon−sulfur fused rings,[6] acenes,[7,8] phthalocyanines,[9,10] polythiophene,[11] and polythienylenevinylenes.[12] Especially, the acene and oligothiophene derivatives represent two of the most heavily studied series of compounds for use as organic semiconductors.[13−16] The field-effect mobility of α,ω-dihexylsexithiophene, one of the

* Co-corresponding author. E-mail: ykim@gsnu.ac.kr (Y.-H.K.).
[†] School of Nano & Advanced Materials Engineering and Engineering Research Institute, Gyeongsang National University.
[‡] Department of Chemistry, Gyeongsang National University.
[§] Gwangju Institute of Science and Technology.
[||] Korea Research Institute of Chemical Technology.

(1) (a) Horowitz, G. *J. Mater. Res.* **2004**, *19*, 1946. (b) Kelley, T. W.; Baude, P. F.; Gerlach, C.; Ender, D. E.; Muyres, D.; Haase, M. A.; Vogel, D. E.; Theiss, S. D. *Chem. Mater.* **2004**, *16*, 4413. (c) Dimitrakopoulos, C. D.; Malenfant, P. R. L. *Adv. Mater.* **2002**, *14*, 99. (d) Bao, Z. *Adv. Mater.* **2000**, *12*, 227.
(2) (a) Baude, P. F.; Ender, D. A.; Haase, M. A.; Kelley, T. W.; Muyres, D. V.; Theiss, S. D. *Appl. Phys. Lett.* **2003**, *82*, 3964. (b) Blanchet, G. B.; Loo, Y.; Rogers, J. A.; Gao, F.; Fincher, C. R. *Appl. Phys. Lett.* **2003**, *82*, 463. (c) Gelinck, G. H.; Huitema, H. E. A.; Van Veenendaal, E.; Cantatore, E.; Schrijnemakers, L.; Van Der Putten, J. B. P. H.; Geuns, T. C. T.; Beenhakkers, M.; Giesbers, J. B.; Huisman, B.; Meijer, E. J.; Benito, E. M.; Touwslager, F. J.; Marsman, A. W.; van Rens, B. J. E.; de Leeuw, D. M. *Nat. Mater.* **2004**, *3*, 106.
(3) (a) Qiu, Y.; Hu, Y.; Dong, G.; Wang, L.; Xie, J.; Ma, Y. *Appl. Phys. Lett.* **2003**, *83*, 1644. (b) Pannemann, C.; Diekmann, T.; Hilleringmann, U. *J. Mater. Res.* **2004**, *19*, 1999.
(4) Halik, M.; Klank, H.; Zschieschang, U.; Schmid, G.; Ponomarenko, S.; Kirchmeyer, S.; Weber, W. *Adv. Mater.* **2003**, *15*, 917.
(5) Katz, H. E.; Dodabalapur, A.; Torsi, L.; Elder, D. *Chem. Mater.* **1995**, *7*, 2238.
(6) Sirringhaus, H.; Friend, R. H.; Li, X. C.; Moratti, S. C.; Holmes, A. B.; Feeder, N. *Appl. Phys. Lett.* **1997**, *71*, 3871.
(7) Ito, K.; Suzuki, T.; Sakamoto, Y.; Kubota, D.; Inoue, Y.; Sato, F.; Tokito, S. *Angew. Chem.* **2003**, *115*, 1191.
(8) Afzali, A.; Dimitrakopoulos, C. D.; Breen, T. C. *J. Am. Chem. Soc.* **2002**, *124*, 8812.
(9) Bao, Z.; Lovinger, A. J.; Dodabalapur, A. *Appl. Phys. Lett.* **1996**, *69*, 3066.
(10) Tang, Q.; Li, H.; He, M.; Hu, W.; Liu, C.; Chen, K.; Wang, C.; Liu, Y.; Zhu, D. *Adv. Mater.* **2006**, *18*, 65.
(11) Ong, B. S.; Wu, Y.; Liu, P.; Gardner, S. *J. Am. Chem. Soc.* **2004**, *126*, 3378.
(12) Fuchigami, H.; Tsumura, A.; Koezuka, H. *Appl. Phys. Lett.* **1993**, *63*, 1372.
(13) Newman, C. R.; Frisbie, C. D.; da Silva Filho, D. A.; Bredas, J.-L.; Ewbank, P. C.; Mann, K. R. *Chem. Mater.* **2004**, *16*, 4436.
(14) Katz, H. E.; Bao, Z.; Gilat, S. L. *Acc. Chem. Res.* **2001**, *34*, 359.
(15) Facchetti, A.; Mushrush, M.; Katz, H. E.; Marks, T. J. *Adv. Mater.* **2003**, *15*, 33.
(16) Hong, X. M.; Katz, H. E.; Lovinger, A. J.; Wang, B.-C.; Raghavachari, K. *Chem. Mater.* **2001**, *13*, 4686−4691.

10.1021/cm070053g CCC: $37.00
Published on Web 06/01/2007

Scheme 1. Synthetic Schemes of Oligomers

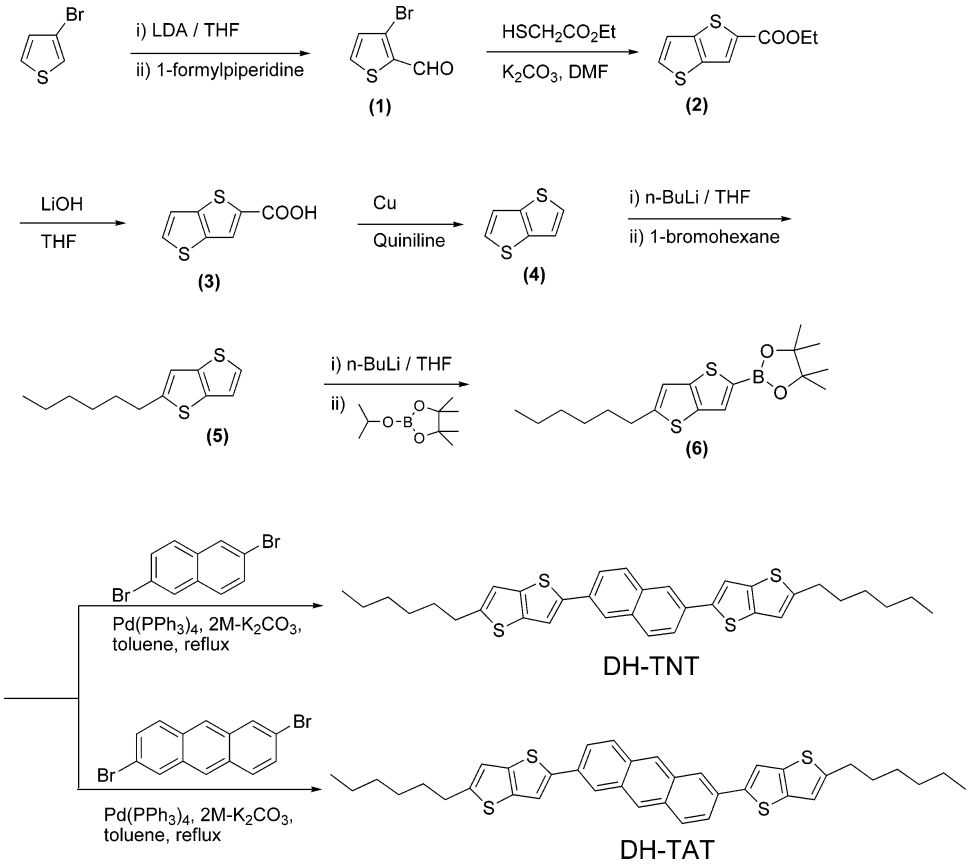

most widely investigated materiala, reaches 0.1 cm^2/Vs depending on the material used for the gate insulator and the fabrication method.[17,18] Pentacene also has good TFT performance (mobilities up to 3.0 cm^2/Vs)[19] due to its planar shape facilitating crystal packing and the extended π-conjugated system over molecules enabling the intermolecular overlap of π-systems. However, chemical instability of pentacene has been restricted in synthesis and thin film deposition as well as commercial application despite their excellent TFT characteristics. Recently, hybrid acene−thiophene molecules, which had good thermal and oxidation stability as well as good TFT characteristics, were reported.[20,21] It was also reported that TFT characteristics could be increased by the substitution of fused thienothiophene instead of bithiophene.[22,23]

To obtain high carrier mobilities without decreasing the chemical stability, it is crucial that the organic molecules be arranged in a specific molecular architecture. Thus, we designed new acene derivatives that are composed of an naphthalene or anthracene core unit and alkylated thienothiophene on both sides. The thienothiophene−naphthalene−thieno-thiophene moiety or thienothiophene−anthracene−thienoyhiophene moiety in designed molecules, which are composed fused aromatics, would be expected to have a suitable HOMO and solid-state structure for use as a p-channel TFT semiconductor. In addition, the barrier to oxidation could be higher than that for pentacene, which usually has oxygen addition across the central ring. In the fused aromatics, the hexyl group is introduced on the α position of sulfur of thienothiophene for the increasing of their capacity for self-assembling into close-packed structures.

In this paper, we report the synthesis and characterization of a series of new organic semiconductors, 2,6-bis(5′-hexyl-thieno[3,2-b]thiophen-2′-yl)naphthalene (DH-TNT) and 2,6-bis(5′-hexyl-thieno[3,2-b]thiophen-2′-yl)anthracene (DH-TAT). The methods for preparing the dihexyl substituted DH-TNT and DH-TAT are outlined in Scheme 1. Thieno[3,2-b]thiophene was synthesized according to the literature procedures starting from 3-bromothiophene.[24] Thieno[3,2-b]thiophene was reacted with *n*-butyllithium and 1-bromohexane to give 2-hexylthieno[3,2-b]thiophene. The lithiated 2-hexylthieno[3,2-b]thiophene was reacted with 2-isopropoxy-4,4,5,5-tetramethyl-1,3,2-dioxaborolane to give 2-(2′-hexyl-5′-thieno[3,2-b]thienyl)-4,4,5,5-tetramethyl-1,3,2-doxaborolane (6). The new dihexyl substituted TNT and TAT

(17) Garnier, F.; Yassar, A.; Hajlaoui, R.; Horowitz, G.; Deloffre, F.; Servet, B.; Ries, S.; Alnot, P. *J. Am. Chem. Soc.* **1993**, *115*, 8716.
(18) Dimitrakopoulos, C. D.; Furman, B. K.; Graham, T.; Hedge, S.; Purushothaman, S. *Synth. Met.* **1998**, *92*, 47.
(19) Klauk, H.; Halik, M.; Zschieschang, U.; Schmid, G.; Radlik, W.; Weber, W. *J. Appl. Phys.* **2002**, *92*, 5259.
(20) Meng, H.; Sun, F.; Goldfinger, M. B.; Jaycox, G. D.; Li, Z.; Marshall, W. J.; Blackman, G. S. *J. Am. Chem. Soc.* **2005**, *127*, 2406.
(21) Merlo, J. A.; Newman, C. R.; Gerlach, C. P.; Kelley, T. W.; Muyres, D. V.; Frits, S. E.; Toney, M. F.; Frisbie, C. D. *J. Am. Chem. Soc.* **2005**, *127*, 3997.
(22) (a) Lim, E.; Jung, B. J.; Shim, H. K. *Macromolecules* **2003**, *36*, 4288. (b) Lim, E.; Jung, B. J.; Lee, J.; Shim, H. K.; Lee, J. I.; Yang, Y. S.; Do, L. M. *Macromolecules* **2005**, *38*, 4531.
(23) Noh, Y. Y.; Azumi, R.; Goto, M.; Jung, B. J.; Lim, E.; Shim, H. K.; Yoshida, Y.; Yase, K.; Kim, D. Y. *Chem. Mater.* **2005**, *17*, 3861.
(24) Fuller, L. S.; Iddon, B.; Smith, K. A. *J. Chem. Soc., Perkin Trans.* **1997**, *1*, 3465.

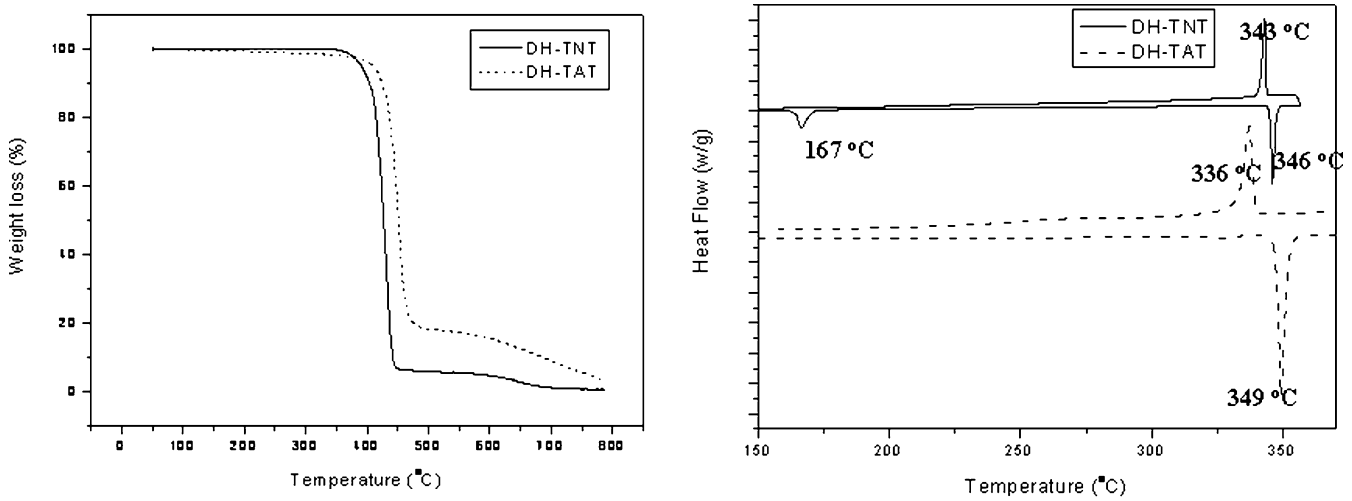

Figure 1. DSC thermograms of DH-TNT and DH-TAT.

were prepared by Suzuki cross coupling reaction with good yield. The obtained oligomers were confirmed by FT-IR and mass and elemental analysis. All the oligomers are soluble in hot aromatic solvent such as chlorobenzene and toluene, etc. The obtained materials were purified by multiple Soxhlet extraction using methanol and toluene. Further purification was then carried out by means of gradient sublimation before the devices were fabricated.

The thermal properties of synthesized oligomers were evaluated by means of thermogravimetric analysis (TGA) and differential scanning calorimetry (DSC) in a nitrogen atmosphere. TGA revealed that the obtained oligomers showed high thermal stability. Five percemt weight loss was observed at 391 °C for DH-TNT and 409 °C for DH-TAT, respectively. In contrast, oligothiophene-based α,ω-dihexylsexythiophene (DH6T**)** decomposes at 320 °C under similar conditions.[25] TGA analysis showed that DH-TAT is more thermally stable than DH-TNT, which may originate from the difference in thermal stability between naphthalene and anthracene. DSC results reveals melting features for the two compounds. In the case of DH-TAT, a single endothermic and exothermic transition was observed at a temperature of 349 and 336 °C, respectively, under heating and cooling cycle. DH-TNT displayed a monotropic LC behavior. In the heating trace, two endothermic peaks at 167 and 346 °C were observed. On the other hand, in the cooling trace, only one exothermic peak at 343 °C was observed. (Figure 1) The thermal responses of oligomers reveal that all oligomers are crystalline and suggest that well-ordered thin films could be formed by thermal evaporation processes.

The optical properties of the oligomers were investigated using UV−vis and photoluminescence (PL) spectroscopies. (Figure 2) The new oligomers exhibited absorption maxima in dilute chloroform solution at 296 and 380 nm for DH-TNT and 344, 412, and 438 nm for DH-TAT. In PL spectra, all compounds exhibited blue fluorescence in solution, but in the thin films, transitions from blue emission to blue-green emission were observed when the films were irradiated with UV light. These transitions may have originated from

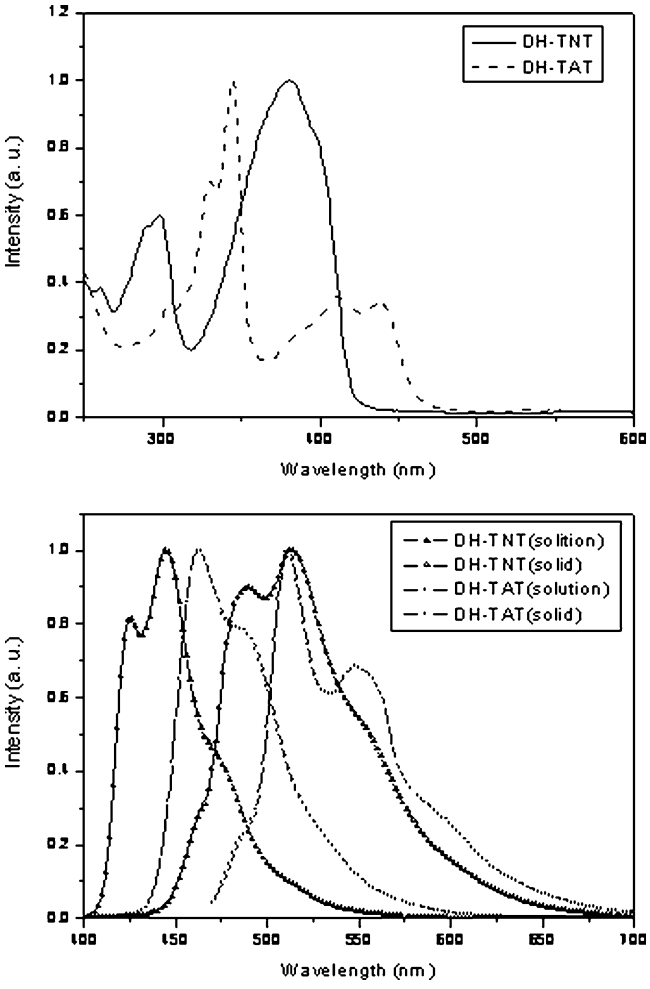

Figure 2. UV−vis and PL spectra of DH-TNT and DH-TAT.

aggregation or excimer formation due to $\pi-\pi^*$ stacking or intermolecular interaction caused by their planar structure.

To understand the charge transport properties and assess the ionization potentials, and the electrochemical stability of the oligomers, we have carried out cyclic voltammetry (CV) measurements on thin films of the oligomers. The electrochemical properties along with the ionization potentials of the oligomers are summarized in Table 1. The oligomers

(25) Inoue, Y.; Tokito, S.; Ito, K.; Suzuki, T. *J. Appl. Phys.* **2004**, *95*, 5795.

Table 1. Electrochemical Properties of Oligomers

oligomer	E_{ox} (V)	E_{re} (V)	HOMO (eV)	LUMO (eV)	bandgap (eV)
DH-TNT	1.00	1.65	5.40	2.75	2.65
DH-TAT	0.85	1.56	5.25	2.84	2.41

present a partially reversible oxidation process at 1.00 and 0.85 V for DH-TNT and DH-TAT, respectively, versus a standard calomel electrode (SCE). The HOMO energy level of oligomers were in the range of 5.25−5.4 eV, resulting in good electrochemical stability. For p-type semiconductors, the majority carriers are holes. For this reason, it is important to reduce the energy barrier between gold electrode and organic semiconductor so that the HOMO level of the p-type semiconductor should be closed to the work function of gold electrode (5.4 eV).[26] Therefore, the determined HOMO levels of the oligomers should match well with the work function of the gold metal. Consequently, the hole injection from the gold source electrode in the p-channel oligomers thin film transistors is expected to be efficient.

The orientation of the thin film was investigated by means of X-ray diffraction (XRD) analysis. Figure 3 shows X-ray diffractograms of DH-TNT and DH-TAT films (∼50 nm) deposited on silicon wafer. (DH-TNT, T_s = RT, 100 °C, and DH-TAT, T_s = RT, 120 °C). The surface of the substrate was pretreated with 1,1,1,3,3,3-hexamethyldisilazane (HMDS) to reduce the surface energy between the oligomer and the SiO_2 interface. The first strong reflection peak of these corresponds exactly to the length of the oligomers (*d*-spacing of 33.2 and 37 Å for DH-TNT and DH-TAT, respectively) and the others are its second, third, and fourth orders, respectively, when we consider the length of the molecular long axis via molecular simulation using Hyper Chem 7.0 (32.6 Å for DH-TNT and 34.7 Å for DH-TAT, respectively). Therefore, the oligomers are considered to be perpendicular to the substrate. As the substrate temperature increased, the XRD patterns showed higher-order reflections with sharp and strong reflection peaks. This indicates that the oligomer films

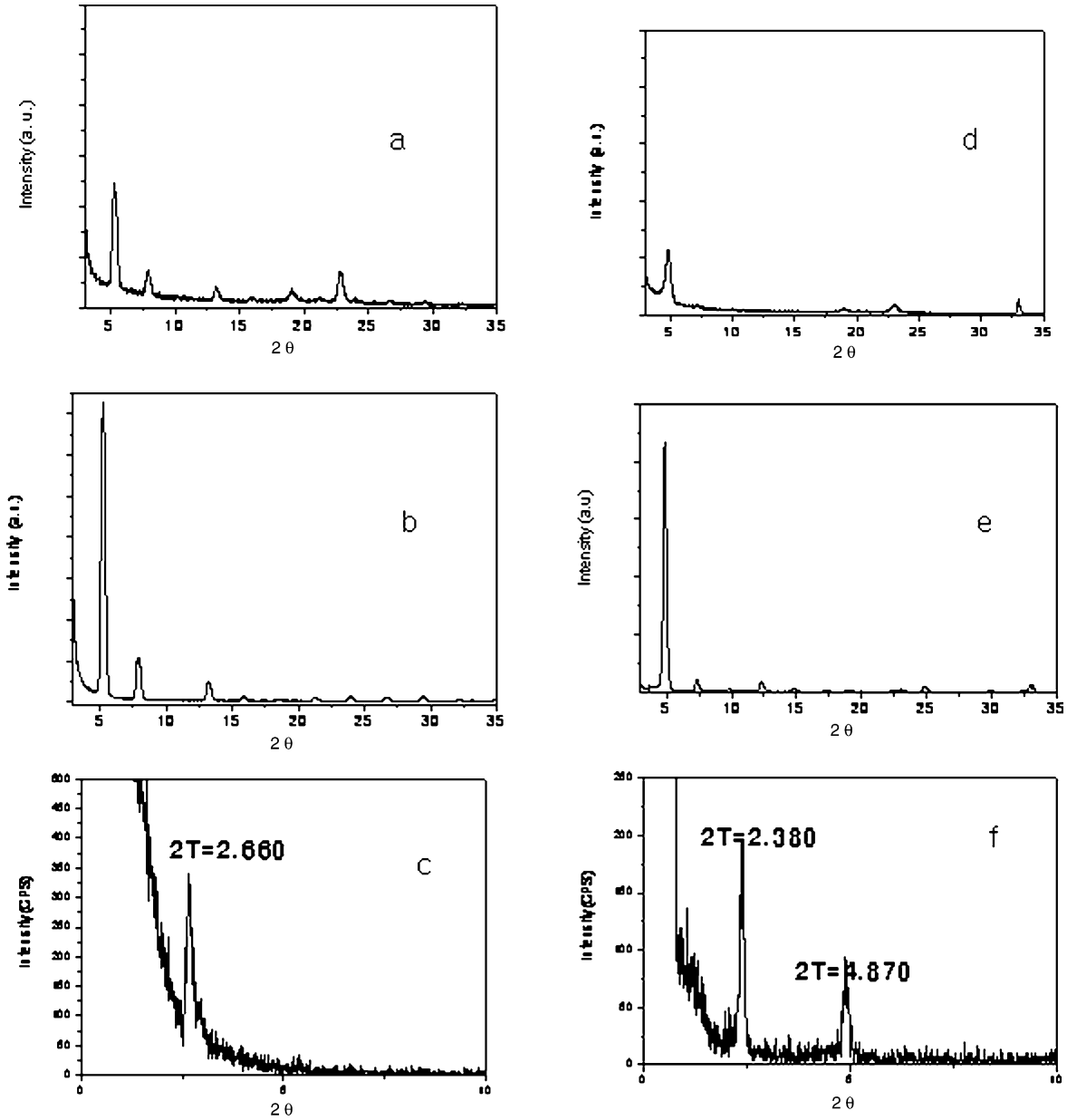

Figure 3. X-ray diffractograms of evaporated thin films of (a) 25, (b) 100, and (c) 100 °C (2T: 0−5) of DH-TNT and (d) 25, (e) 120, and (f) 120 °C (2T: 0−5) of DH-TAT (∼50 nm thickness, treated HMDS on SiO_2).

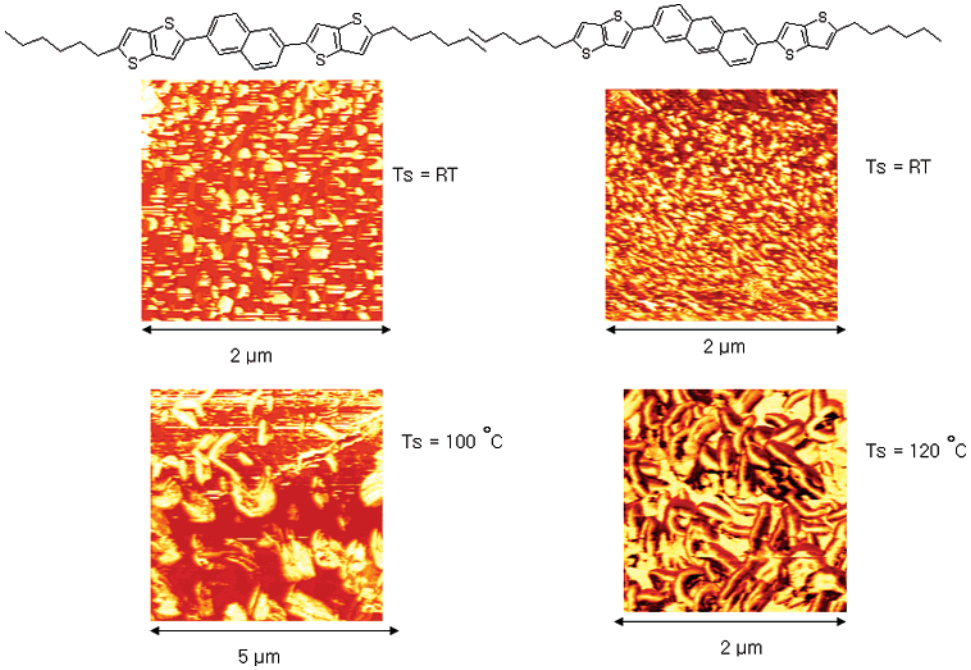

Figure 4. AFM images (phase) of (a) 25 and (b) 100 °C of DH-TNT and (c) 25 and (d) 120 °C of DH-TAT (~50 nm thickness, treated HMDS on SiO_2).

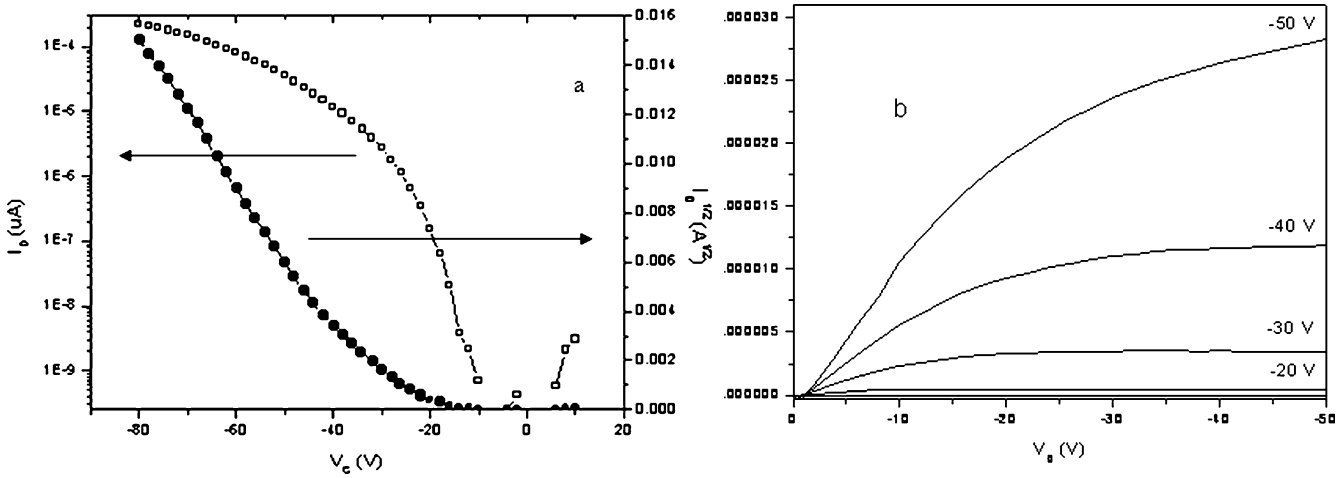

Figure 5. (a) Drain current (ID) versus gate voltage (VG) characteristics of the DH-TNT OFET at a Drain current of −80 V. (b) Drain current (I_D) vs drain-source voltage (V_D) characteristics of the DH-TNT OFET at different gate voltage (V_G).

with a high degree of lamellar ordering and crystallinity are formed at the higher temperatures. Such film morphology is known to be a favorable structure in polycrystalline films in terms of achieving a high mobility. AFM images of the oligomers are shown in Figure 4. It is clearly seen in both cases that polycrystalline films are formed. DH-TAT shows large needlelike crystals, whereas DH-TNT does not form large needlelike crystals. In spite of the difference in the morphology features, in both cases, we have full covering of the substrate with the material and good network interconnection between the crystallites, which is probably responsible for large charge-carrier mobility, measured in OTFTs.

OTFTs were fabricated using thin films of oligomers as active layers, and their electrical properties were characterized. The mobility (μ_{FET}) and threshold voltage (V_{TH}) of the OFETs where obtained from eq 1 for saturation regimes.

$$I_D^{sat} = (W/2L)\mu_{FET}C_i(V_G - V_{TH})^2 \qquad (1)$$

Where L is the channel length, W is the channel width, and C_i is the capacitance per unit area of the gate dielectric layer (C_i = 10 nF/cm^2 for 300 nm thick SiO_2). The output characteristics showed very good saturation behavior and clear saturation currents that are quadratic to the gate bias.

The calculated initial mobilities of the devices that deposited at room temperature (T_s = 25 °C) by plotting $I_D^{1/2}$ vs V_G were in range of 0.052−0.059 cm^2/Vs. The best device performances were obtained when DH-TAT was deposited at T_s = 120 °C on HMDS-treated SiO_2, with a hole mobility of 0.14 cm^2/Vs, an on/off current ratio of 6.3 × 10^6, and a good threshold voltage of −14 V. The typical field-effect transistor curves and transfer characteristics using DH-TAT as an active semiconductor are presented in Figure 5. Table 2 summarizes the field-effect mobilities as well as the on/off current ratios and the threshold voltages obtained with DH-TNT and DH-TAT as active semiconductor layers deposited at different substrate temperatures. As shown in Table 2, the mobilities increase with increasing substrate temperature. It seems that molecular ordering and/or crystal-

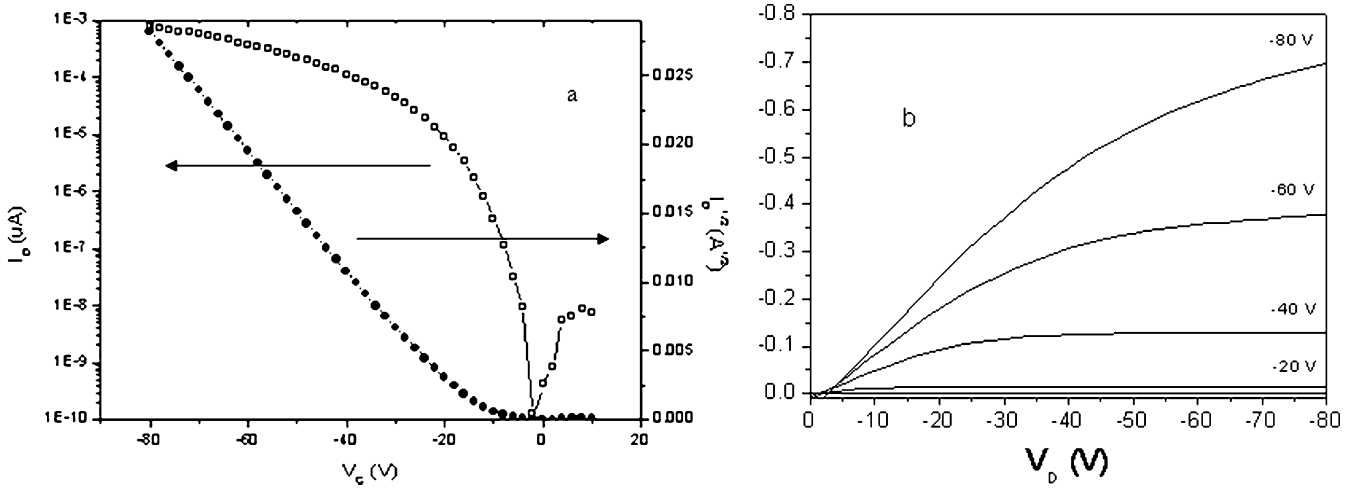

Figure 6. (a) Drain current (ID) versus gate voltage (VG) characteristics of the DH-TNT OFET at a Drain current of −80 V. (b) Drain current (I_D) vs drain-source voltage (V_D) characteristics of the DH-TAT OFET at different gate voltage (V_G).

Table 2. TFT Characteristics of Oligomers

oligomer	T_s (°C)	μ_{FET} (cm^2/Vs)	V_{TH} (V)	I_{OFF} (A)	I_{ON}/I_{OFF}
DH-TNT	25	0.052	−30	4.9×10^{-11}	3.2×10^6
	100	0.084	−26	2.56×10^{-10}	8.8×10^5
DH-TAT	25	0.059	−18.6	1.24×10^{-9}	5.9×10^4
	120	0.14	−14	1.25×10^{-10}	6.3×10^6
	150	0.07	−14	2.3×10^{-9}	5.9×10^4

linity of oligomer thin film was improved at the higher substrate temperature. The results can be proved by the results of XRD and AFM. Compared with the naphthalene and anthracene derivative, DH-TAT has a higher mobility than that of DH-TNT. It seems that the conjugation length of DH-TAT is higher than that of DH-TNT and the hole-injection energy barrier of DH-TAT is lower than that of DH-TNT because of its higher HOMO level compared with that of DH-TAT. The results of OTFT using obtained oligomers indicate that the oligomerization is effective for developing high-mobility organic semiconductors.

In conclusion, we fabricated OTFTs based a series of new organic semiconductors that we designed and synthesized. The oligomers are highly thermally stable, and XRD patterns and AFM revealed that these films, grown by vacuum deposition, are highly crystalline. The compounds exhibit excellent field-effect performances, with mobilities as high as 0.14 cm^2/Vs and an on/off ratio up to 6.3×10^6. The introduction of hexylthieno[3,2-b]thiophene favored the high electron density of the molecules, which facilitates the charge transport through $\pi-\pi^*$ stacking of the molecules. Studies of the FET mobility with different oligomer conjugation lengths, such as those of naphthalene and anthracene, indicate that there may exist some relationships between the mobility, the conjugation length, and the deposition temperatures.

Experimental Section

Materials. 3-Bromothiophene and ethyl 1-sulfanyl acetate were purchased from TCI. *n*-Butyllithium, diisopropyl amine, *N*-formylpiperidine, *N*-bromosuccinimide (NBS), 1-bromohexane, copper powder, quinoline, and 2-isopropoxy-4,4,5,5-tetramethyl-1,3,2-dioxaborolane were purchased from Aldrich. Tetrakis(triphenylphosphine)palladium was purchased from Strem. 2,6-dibromonaphthalene was purchased from Lancaster. All reagents purchased commercially were used without further purification. Tetrahydrofuran (THF) and diethyl ether were dried over sodium/benzophenone. 2,6-Dibromoanthracene was prepared with methods from the literature.[7]

Measurements. A Genesis II FT-IR spectrometer was used to record IR spectra. ^{1}H NMR and ^{13}C NMR spectra were recorded with the use of Avance 300 and DRX 300 MHz NMR Bruker spectrometers, and chemical shifts are reported in units of parts per million with tetramethylsilane as internal standard. Thermogravimetric analysis (TGA) was performed under nitrogen on a TA instrument 2050 thermogravimetric analyzer. The sample was heated using a 10 °C/min heating rate from 50 to 800 °C. Differential scanning calorimeter (DSC) was conducted under nitrogen on a TA Instruments 2100 differential scanning calorimeter. The sample was heated at 10 °C/min from 30 to 300 °C. The mass spectrum was measured by a Jeol JMS-700 mass spectrometer. UV−vis absorption spectra and photoluminescence (PL) spectra were measured by Perkin-Elmer LAMBDA-900 UV−vis−NIR spectrophotometer and LS-50B luminescence spectrophotometer, respectively. Cyclic voltammograms of the oligomers were recorded on an epsilon E3 at a room temperature in a 0.1 M solution of tetrabutylammonium perchrolate (Bu_4NClO_4) in acetonitrile under nitrogen gas protection at a scan rate of 50 mV/s. A Pt wire was used as the counter electrode and a $Ag/AgNO_3$ electrode as the reference electrode.

Device Fabrication. A thin film organic semiconducting layer (about 50 nm measured by a quartz-crystal thickness monitor) was deposited on a SiO_2 (300 nm, 10 nF/cm^2) surface on a heavily doped silicon wafer as the gate electrode. The SiO_2 surface were pretreated with 1,1,1,3,3,3-hexamethyldisilazane (HMDS). After evaporation, the OTFTs were completed by evaporating gold through a shadow mask to form source and drain electrodes on the semiconducting thin films as a top contact geometry. This device has a channel length and width of 20 μm and 5 mm, respectively. The FETs characteristics were measured with a KEITHLEY 4200 semiconductor characterization system at an air atmosphere.

Synthesis. *2-Hexylthieno[3,2-b]thiophene (5).* *n*-Butyllithium (23.1 g, 0.083 mol) was added dropwise to a solution of thieno-[3,2-b]thiophene (13 g, 0.093 mol) in THF (200 mL) at −78 °C. One hour after addition, 1-bromohexane (15.3 g, 0.093 mol) was added to the solution. The reaction mixture was then warmed to room temperature, stirred for another 5 h, and poured into water. The mixture was extracted with ether and dried over magnesium

(26) Ando, S.; Nishida, J.; Fujiwara, E.; Tada, H.; Inoue, Y.; Tokito, S.; Yamashita, Y. *Chem. Mater*. **2005**, *17*, 1261.

sulfate, and the solvent was evaporated. The product was purified by vacuum distillation. Yield: 10.3 g (55%), bp: 120−124 °C/1 mmHg, ^{1}H NMR (300 MHz, $CDCl_3$, ppm): 7.31 (d, 1H), 7.23 (d, 1H), 6.99 (s, 1H), 2.94 (t, 2H), 1.72−1.81 (m, 2H), 1.36−1.49 (m, 6H), 0.95 (t, 3H).

*2-(2′-Hexyl-5′-thieno[3,2-b]thienyl)-4,4,5,5-thtramethyl-1,3,2-doxaborolane (**6**).* To a solution of compound **5** (10 g, 44.6 mmol) in THF (150 mL) at −78 °C was added dropwise *n*-butyllithium (13.6 g, 49.02 mmol). After the mixture had been stirred at −78 °C for 1 h, 2-isopropoxy-4,4,5,5-tetramethyl-1,3,2-dioxaborolane (9.9 g, 53.5 mmol) was added to the mixture, and the resulting mixture was stirred at −78 °C for 1 h and then warmed to room temperature and further stirred for overnight. The mixture was poured into water, extracted with diethylether, and then dried over $MgSO_4$. The solvent was removed by rotary evaporation; the yellow oil was obtained after a flash column chromatography using hexane: ethylacetate (10:1) as eluent. Yield: 6.3 g (41%). Mp: 64 °C. FT−IR (KBr, cm^{-1}): 2950 (aromatic C−H), 2853 (aliphatic C−H), 849 (C−S). ^{1}H NMR (300 MHz, $CDCl_3$, ppm): 7.69 (s, 1H), 6.99 (s, 1H), 2.89 (t, 2H), 1.69−1.76 (m, 2H), 1.31−1.43 (m, 18H), 0.88−0.93 (m, 3H). ^{13}C NMR (300 MHz, $CDCl_3$, ppm): aromatic C; 151.5, 145.2, 138.8, 129.1, 116.3, aliphatic C; 31.5, 31.4, 31.3, 28.7, 24.7, 22.5, 14.02.

2,6-Bis(5′-hexyl-thieno[3,2-b]thiophen-2′-yl)naphthalene (DH-TNT). To a solution of compound **6** (2.8 g, 8.04 mmol) and 2,6-dibromonaphthalene (1 g, 3.5 mmol) dissolved in toluene (50 mL) was added an aqueous 2 M potasium carbonate solution (20 mL). The mixture was bubbled with nitrogen for 30 min. Tetrakis-(triphenylphosphine)palladium(0) (0.08 g, 2% mol) was then added. The mixture was heated to 90 °C for 48 h under a nitrogen atmosphere. The reaction mixture was cooled to room temperature and poured into methanol (400 mL) and aqueous 2 N HCl (200 mL). The orange precipitate was filtered off and washed with water, methanol, and then three times with acetone to remove the starting material as well as the monosubstituted byproduct. The crude product was purified by Soxhlet extraction with methanol and toluene. Yield: 1.65 g (82.5%). Mp: 346 °C (DSC). FT−IR (KBr, cm^{-1}): 3071 (aromatic C−H), 2849 (aliphatic C−H), 800 (C−S). MS (EI) *m*/*z*: 572 (M^+). Anal. Cacld for $C_{34}H_{36}S_4$: C, 71.28; H, 6.33. Found: C, 71.55; H, 6.43.

2,6-Bis(5′-hexyl-thieno[3,2-b]thiophen-2′-yl)anthracene (DH-TAT). DH-TAT was prepared using the same method as described for DH-TNT using 2,6-dibromoanthracene (1 g, 2.9 mmol) and compound **6** (2.4 g, 6.8 mmol). Yield: 1.27 g (70%). Mp: 349 °C (DSC). FT−IR (KBr, cm^{-1}): 3056 (aromatic C−H), 2848 (aliphatic C−H), 800 (C−S). MS (EI) *m*/*z*: 622 (M^+). Anal. Cacld for $C_{38}H_{38}S_4$: C, 73.26; H, 6.15. Found: C, 73.09; H, 6.38.

Acknowledgment. This research was supported by the 21st Century Frontier R&D Program funded by the Ministry of Science and Technology of the Korean Government and the Korea Research Foundation Grant KRF-2000-005-D00251.

Supporting Information Available: FT−IR and mass spectra of DH-TNT and DH-TAT. This material is available free of charge via the Internet at http://pubs.acs.org.

CM070053G